

Adsorption of Pb, Ni and Zn by coastal soils: Isothermal models and kinetics analysis

Tatiana Minkina ^a, Tatiana Bauer ^a, Oleg Khroniuk ^a, Ekaterina Kravchenko ^{a,*},
David Pinsky ^b, Anatoly Barakhov ^a, Inna Zamulina ^a, Elizabeth Latsynnik ^a,
Svetlana Sushkova ^a, Yao Jun ^c, Coşkun Gülser ^d, Rıdvan Kızılkaya ^d

^a Southern Federal University, Rostov-on-Don, 344090, Russia

^b Institute of Physicochemical and Biological Problems of Soil Science, Russian Academy of Sciences, 142290 Pushchino, Russia

^c China University of Geosciences, School of Water Resources and Environment, Beijing, China

^d Ondokuz Mayıs University, Faculty of Agriculture, Department of Soil Science and Plant Nutrition, Samsun, Türkiye

Abstract

Article Info

Received : 21.04.2024

Accepted : 24.10.2024

Available online: 04.11.2024

Author(s)

T.Minkina



T.Bauer



O.Khroniuk



E.Kravchenko *



D.Pinsky



A.Barakhov



I.Zamulina



E.Latsynnik



S.Sushkova



Y.Jun



C.Gülser



R.Kızılkaya



Coastal areas are facing increasing heavy metal pollution as a result of various anthropogenic activities, posing a serious threat to ecosystems. Modeling and understanding the sorption behavior of heavy metals in soils are essential for assessing their mobility and risk in the coastal landscapes. The aim of this study was to examine the adsorption behavior of Pb²⁺, Ni²⁺, and Zn²⁺ by common soil types of the Lower Don and the Taganrog Bay coast in Russia to better understand their potential environmental implications. The soil capacities for heavy metal adsorption and retention were determined using isothermal models. The maximum adsorption capacity and the binding strength parameter for the heavy metals were calculated, revealing significant differences among the soils. Haplic Chernozem emerged with superior values, while Gleyic Solonchak Sulfidic and Umbric Fluvisol trailed the lowest. All soils exhibited a greater adsorption capacity and binding strength for Pb compared to the other metals. The influence of soil characteristics on sorption and retention was also examined. The Pseudo-second-order model provided a more accurate description of the adsorption kinetics of heavy metals by the studied soils. The co-presence of metals in the system affected their sorption by the soils due to competition: soils adsorbed fewer metals but retained them more strongly. These findings are important for developing effective strategies to reduce heavy metal pollution in coastal ecosystems.

Keywords: Heavy metals, Soils, Individual and Competitive adsorption, Adsorption capacity, Binding strength, Kinetics

* Corresponding author

© 2025 Federation of Eurasian Soil Science Societies. All rights reserved

Introduction

The growth in the Earth's population and the industrialization of human lifestyles inevitably lead to environmental pollution from anthropogenic emissions (Zamora-Ledezma et al., 2021). Soils, nature's universal filters, possess the remarkable ability to absorb, retain, and transform myriad pollutants into benign forms, yet they remain acutely vulnerable to anthropogenic contamination (Vega et al., 2006; Pinski et al., 2023). Among the most dangerous pollutants for soils are heavy metals (HMs), whose formidable toxicity, tenacity against degradation, propensity for biological accumulation, and pervasive presence render them particularly hazardous (Tepanosyan et al., 2018; Bai et al., 2019). These elements can infiltrate the food chain, jeopardizing the delicate balance of ecosystems and endangering human health alike (Li et al.,

doi : <https://doi.org/10.18393/ejss.1579168>

globe : <https://ejss.fesss.org/10.18393/ejss.1579168>

Publisher : Federation of Eurasian Soil Science Societies

e-ISSN : 2147-4249

2023). Through this interconnected web of life, the insidious threat of heavy metals looms, casting a shadow over both our environment and the well-being of future generations.

To assess the potential mobility and fate of HMs within naturally contaminated soils, it is crucial to predict both the timing and magnitude of leaching events. This endeavor calls for a thorough exploration of patterns and mechanisms underpinning HM sorption and stabilization within the soil matrix (Liu et al., 2023; Cao et al., 2024). Sorption emerges as a pivotal factor dictating the fate and transport of HMs within ecosystems (Degryse et al., 2009; Bauer et al., 2018; Zwolak et al., 2019). The phenomenon of adsorption governs HM leaching from soil, with the extent of leaching intricately linked to the adsorption equilibrium, which describes the distribution of metals between the solid and liquid phases (Komuro and Kikumoto, 2024). A suite of sorption equilibrium models, including the linear, Freundlich, Langmuir, and Dubinin-Radushkevich equations, have been articulated, with the partitioning coefficient influenced by factors such as pH, temperature, Fe/Mn oxide content, and clay and silt content (Das et al., 2014; Diagboya et al., 2015). Furthermore, numerical models, such as the Pseudo-first order model (PFO, Lagergren model) and the Pseudo-second order model (PSO), have been proposed (Ho and McKay, 1999). These models capture sorption kinetics characterized by rapid sorption at the initial stage, followed by a slower rate later on.

The mechanisms governing HM sorption by soils are remarkably intricate, shaped by a multitude of factors. These include pH levels, ionic strength of the solution, the presence of competing ions, the composition and availability of soil sorption sites, as well as the potential for precipitation on soil particle surfaces and within the liquid phase in the presence of components such as carbonates, phosphates, organic matter, silicates, oxides, and hydroxides (Jalali and Moharrami, 2007; Sipos et al., 2008; Usman, 2008; Fisher-Power et al., 2016; Bauer et al., 2022).

Soil contamination frequently entails the concurrent presence of multiple HMs. In such scenarios, the dynamics and behavior of these HMs are dictated by the competition for sorption sites (Vega et al., 2006; Li et al., 2023). Research on the quantitative patterns of HM sorption by soils has revealed that metals like Ni, Pb, and Zn can compete for adsorption sites on soil particles (Lu and Xu, 2009; Akrawi et al., 2021; Umeh et al., 2021; Kravchenko et al., 2024). Ultimately, the composition and properties of the soil stand as the foremost determinants of HM adsorption (Jalali and Moharrami, 2007; Imoto and Yasutaka, 2020; Daramola et al., 2024).

The exploration of soil sorption capacity within coastal realms assumes profound significance, for these vibrant regions serve as conduits of both natural and anthropogenic transport and deposition (Ward et al., 2020). During these processes, coastal soils embody a protective buffer, sequestering HMs and threatening human health (Yu et al., 2021). The functioning of seaports and shipping are prominent sources of HM pollution in coastal ecosystems, leading to their degradation (Konstantinova et al., 2024). Moreover, these coastal zones provide invaluable ecosystem services and cradle nearly 40% of the global population dwelling within 100 km of the shoreline (Kulp and Strauss, 2019).

Among the most densely populated and heavily utilized areas in southern Russia, the Lower Don region and the coast of the Taganrog Bay of the Azov Sea are engaged in a perilous interplay of anthropogenic pressure on the soil degradation, resulting in a concerning accumulation of priority HMs such as Pb, Ni, and Zn (Konstantinova et al., 2023). These HMs rank among the foremost pollutants to infiltrate the environment, with adverse effects on ecosystems (Najamuddin et al., 2024). The aim of this study is to assess the patterns and mechanisms of mono- and poly-elemental sorption, as well as the sorption kinetics of Pb, Ni, and Zn by coastal soils with varying compositions and properties: Umbric Fluvisol, Gleyic Solonchac Sulfidic, and Haplic Chernozem.

Material and Methods

Soil sampling and analysis

The objects of investigation were the soils of various genesis (zonal, azonal and intrazonal) of the Lower Don and along the coast of the Taganrog Bay (Rostov region, Russia). The soils were classified as Umbric Fluvisol, Gleyic Solonchac Sulfidic and Haplic Chernozem (IUSS, 2015). Soil samples were meticulously collected to a depth ranging from 0 to 20 cm, then air-dried at ambient temperature before being combined and sieved through a 1 mm sieve. The main primary physical and chemical characteristics of the studied soils were assessed employing a suite of analytical methods: pH of soil suspension in water was measured according to ISO 10390:2005; the content of soil organic matter (SOM) content was measured according to the sulfochromic oxidation, ISO 14235: 1998; the carbonates content was determined using a Scheibler

apparatus, ISO 10693: 1995; cation exchange capacity (CEC) and exchangeable cations Ca^{2+} and Mg^{2+} were evaluated with by hexamminecobalt trichloride solution in accordance with ISO 23470: 2018. The particle size distribution was determined using the pipette method with the pyrophosphate procedure preparation (Shein, 2009). The total elemental composition (Si, Fe, Al) in the soils was determined by X-ray fluorescent (XRF) scanning spectrometer SPECTROSCAN MAK-S-GV.

An X-ray diffractometry using DRON-7 diffractometer in Cu-K α -filtered radiation was used to determine the mineralogical composition of the clay fraction of soils with a size less than 1 μm . For this purpose, the silt fraction was meticulously isolated from the studied soils (0-20 cm layer) by the sedimentation method according to (Chizhikova et al., 2018). After removing carbonates, the samples were kneaded twice (for 20 min) with a rubber pestle in a paste-like state. The soil samples were transferred to glass containers (3 L) with marks, in which the suspension was elutriated. The soil particles were separated into fractions by immersing the siphon to different depths, draining the liquid at certain intervals into receiving vessels. Upon completion of the elutriation, the suspensions of the soil fractions, except for the silt fraction, were dried and weighed. Concentrated CaCl_2 was added to the vessels with the liquid containing the silt fraction ($<1 \mu\text{m}$) for coagulation, and the highly dispersed particles were precipitated using a centrifuge.

Batch adsorption experiments

The metal adsorption on the soils was studied using a batch experiment. The adsorption experiments were performed in 150 mL Erlenmeyer flasks at 25°C. The Pb^{2+} , Ni^{2+} and Zn^{2+} solutions were prepared by dissolving its nitrate salt in deionized water. The initial concentrations of HMs in the solution were 0.05; 0.08; 0.1; 0.3; 0.5; 0.8 and 1.0 $\text{mM}\cdot\text{L}^{-1}$. The studied metal solutions contained either one metal or all three metals simultaneously. Five grams of the soil and 50 mL of HMs solution were added to the flasks. The initial pH of the solutions was adjusted using a dilution of 0.01 M KOH and 0.1 M HNO_3 solution. The flasks were sealed with silicon caps and shaken at 200 rpm in a rotary shaker for 1 h and then left in a calm state for 24 h to reach apparent equilibrium. Preliminary studies (Burachevskaya et al., 2023) showed that an apparent adsorption equilibrium was reached within 24 h. After the experiment, the metal ion concentrations remaining in the filtrate were determined using an atomic absorption spectrophotometer (AAS, The MGA-915 AA, Lyumeks, Russia). The amount of metal adsorbed per gram of soil (C_{ad} , $\text{mM}\cdot\text{kg}^{-1}$) and the efficiency of adsorption (% adsorbed) were determined using equations (1) and (2), respectively (Daramola et al., 2024):

$$C_{\text{ad}} = \frac{(C_i - C_{\text{eq}}) \times V}{m}, \quad (1)$$

$$\% \text{ adsorbed} = \frac{C_i - C_{\text{eq}}}{C_i} \cdot 100, \quad (2)$$

where C_i и C_{eq} are initial and equilibrium metal solution concentrations, $\text{mM}\cdot\text{L}^{-1}$; V is the volume of the solution, mL; m is the mass of the adsorbent, kg. The information gathered was used to create the adsorption isotherms plot ($C_{\text{eq}} - C_{\text{ad}}$).

Adsorption isotherm and kinetic models

Thermodynamic models

The simple Langmuir (3), Freundlich (4) and Dubinin-Radushkevich (Vodyanitskii et al., 2000) (5) models were applied to describe the adsorption characteristics:

$$C_{\text{ad}} = C_{\infty} K_L C_{\text{eq}} / (1 + K_L C_{\text{eq}}), \quad (3)$$

$$C_{\text{ad}} = K_F C_{\text{eq}}^{1/n}, \quad (4)$$

$$C_{\text{ad}} = C_{\infty} \exp(-B\varepsilon^2), \quad (5)$$

where C_{ad} is the amount of absorbed metal per unit weight of adsorbent, C_{∞} is the maximum adsorption capacity for the metal, $\text{mM}\cdot\text{kg}^{-1}$; K_L is the constant of the Langmuir model related to the affinity of the binding sites (Cui et al., 2016), $\text{L}\cdot\text{mM}^{-1}$; C_{eq} is the concentration of metal at equilibrium, $\text{mM}\cdot\text{L}^{-1}$; K_F is the Freundlich adsorption constant, $\text{L}\cdot\text{kg}^{-1}$; $1/n$ is the Freundlich exponent related to adsorption intensity (Cui et al., 2016); B is a constant related to the mean free energy of sorption per mole of the adsorbate $\text{mol}^2\cdot\text{kJ}^{-2}$; ε is Polanyi potential, which is equal to $RT \ln[KC_p / (1 + KC_{\text{eq}})]$, where K is an empirical parameter which is necessary for straightening experimental curves and obtaining quantitative values.

The Gibbs free energy (ΔG) was calculated using the equation (6):

$$\Delta G = - RT \ln K_L, \quad (6)$$

where R is the gas constant, equals to $8.31 \text{ J}\cdot\text{mol}^{-1}\cdot\text{K}^{-1}$; T is the absolute temperature, K ; K_L is the Langmuir constant.

To calculate the binding energy in equation (5), Hobson's formula (1969) is used for the average energy value (7):

$$E = B^{-1/2} / \sqrt{2} \quad (7)$$

Kinetic models

In order to investigate the mechanisms involved during the adsorption processes, a study was conducted to examine the dynamics of HM adsorption by the studied soil types. The concentration of HM in the initial solution with a volume of 50 mL was $0.5 \text{ mM}\cdot\text{L}^{-1}$. Soil weighing 5 g was added to the system. The interaction times of the suspensions were 1, 2, 5, 15, 30, 60, 180, 360 and 1440 minutes, with constant stirring on a shaker. The models of pseudo-first order and pseudo-second order (Ho and McKay, 1999) were used to describe the kinetics of adsorption and identify the limiting stage of the process.

$$Q_t = Q_e (1 - e^{-k_1 t}), \quad (8)$$

$$Q_t = \frac{k_2 Q_e^2 t}{1 + k_2 Q_e t}, \quad (9)$$

where Q_e and Q_t are the amount of sorbed metal per unit mass of the sorbent in equilibrium (the value is determined empirically) and at time t (min), $\text{mM}\cdot\text{kg}^{-1}$; K_1 is the sorption rate constant of the pseudo-first order model, min^{-1} , K_2 is the sorption rate constant of the pseudo-second order model, $\text{kg}\cdot\text{mM}^{-1}\cdot\text{min}^{-1}$.

Statistical analysis

The experiments on adsorption isotherms and kinetics were performed in triplicate, and the standard deviation error bars in the graphs are from 3 replicates. All the calculation data were processed using Origin 2019® software. The R^2 values were used to compare the performance of the Langmuir, Dubinin-Radushkevich, and Freundlich models.

Results and Discussion

Characteristics of studied soils

The main physicochemical properties of the studied soils are given in Table 1. The soils were slightly alkaline. The CaCO_3 content varied from 1.1 to 7.6%. The SOM content ranged from 1.4 to 3.1%. The sum of exchangeable cations of Ca^{2+} and Mg^{2+} varied from 2.0 to $32.7 \text{ cmol}(+)/\text{kg}$. The content of the physical clay fraction (particle size $<10 \mu\text{m}$) in the studied soils ranged from 21.4 to 47.3%, and that of clay particles ($<1 \mu\text{m}$) was 10.5-24.0%. The mineralogy of the soils and their silt fractions indicates that smectite and hydrosludes are dominant. Kaolinite and chlorite are found in smaller amounts in all samples (Table 2).

Table 1. Physicochemical properties of studied soils, layer 0-20 cm

pH	CaCO_3 (%)	SOM (%)	Ca^{2+} , $\text{cmol}(+)/\text{kg}$	Mg^{2+} , $\text{cmol}(+)/\text{kg}$	$\Sigma\text{Ca}^{2+}+\text{Mg}^{2+}$, $\text{cmol}(+)/\text{kg}$	SiO_2 (%)	Fe_2O_3 (%)	Al_2O_3 (%)	Physical clay (particle size $<10 \mu\text{m}$)	Clay (particle size $<1 \mu\text{m}$)
Umbric Fluvisol										
8.1	7.6	1.4	1.1	16.7	2.0	18.7	71.7	3.0	21.4	10.5
Gleyic Solonchac Sulfidic										
7.9	1.1	1.7	21.0	2.2	23.2	45.3	4.9	10.1	36.1	20.2
Haplic Chernozem										
7.5	1.9	3.1	26.9	5.8	32.7	68.5	4.5	11.0	47.3	24.0

Table 2. Total content of dominant clay minerals in studied soils and their silt fractions

Studied soil	Hydrosludes (%)		Smectite phase (%)		Kaolinite + Chlorite (%)		Quartz (%)
	In soil as a whole	In fraction $<1 \mu\text{m}$	In soil as a whole	In fraction $<1 \mu\text{m}$	In soil as a whole	In fraction $<1 \mu\text{m}$	
Umbric Fluvisol	4.6	34.0	5.8	49.0	2.1	17.0	49.5
Gleyic Solonchac Sulfidic	14.7	66.0	2.9	13.0	4.7	21.0	40.6
Haplic Chernozem	7.8	32.0	13.2	54.0	3.4	14.0	30.1

Individual adsorption of HMs by soils

Adsorption isotherms

Figure 1 illustrates the efficiency of individual HM adsorption by the studied soils. At initial concentrations of HM ions in solution reaching up to 1.0 mM L^{-1} , the soils exhibited notable sorption percentages: Pb^{2+} – 91.42–99.64%, Ni^{2+} – 42.00–91.33%, and Zn^{2+} – 31.4–90.0%. As the concentration of the initial solutions escalated, the percentage of Pb^{2+} sorbed by Gleyic Solonchak Sulfidic and Haplic Chernozem soils remained nearly constant at around 99.6%, while in Umbric Fluvisol, this value decreased to 91.42%. The sorption capacity of the soils for Ni^{2+} and Zn^{2+} , in all cases, followed the hierarchy: Haplic Chernozem > Gleyic Solonchak Sulfidic \geq Umbric Fluvisol. This highlights the different buffer capacities of the soils and, consequently, the varying strengths of metal cation retention in different soil types. It further reveals the intricate interactions between adsorbed cations and the soils, as well as changes in the mechanisms of Ni and Zn adsorption by the soil absorption complex (SAC) as the metal ions concentration in the solution increases. Table 3 and Figure 2 present the data on the adsorption of Pb^{2+} , Ni^{2+} and Zn^{2+} cations by Umbric Fluvisol, Gleyic Solonchak Sulfidic and Haplic Chernozem.

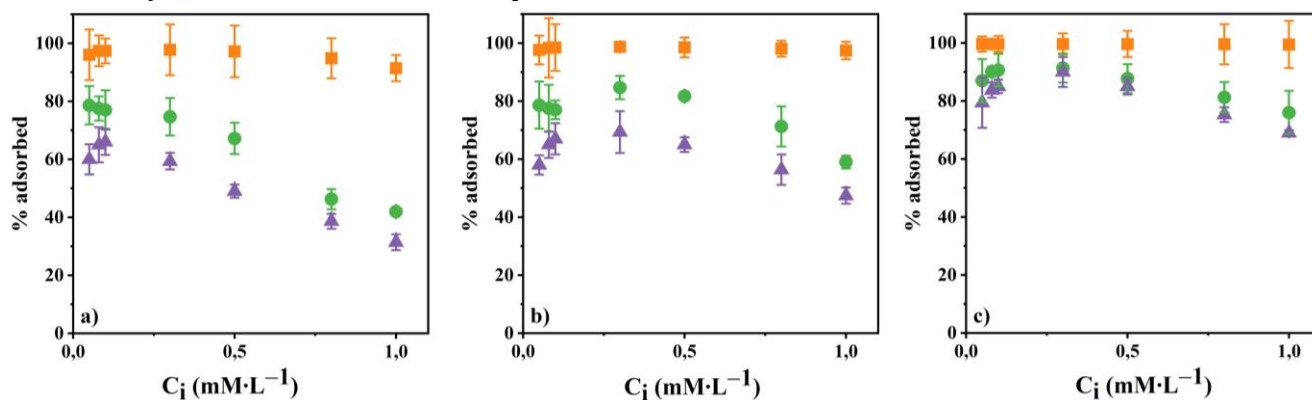


Figure 1. The efficiency of individual adsorption (% adsorbed) of HMs by the Umbric Fluvisol (a), Gleyic Solonchak Sulfidic (b) and Haplic Chernozem (c)

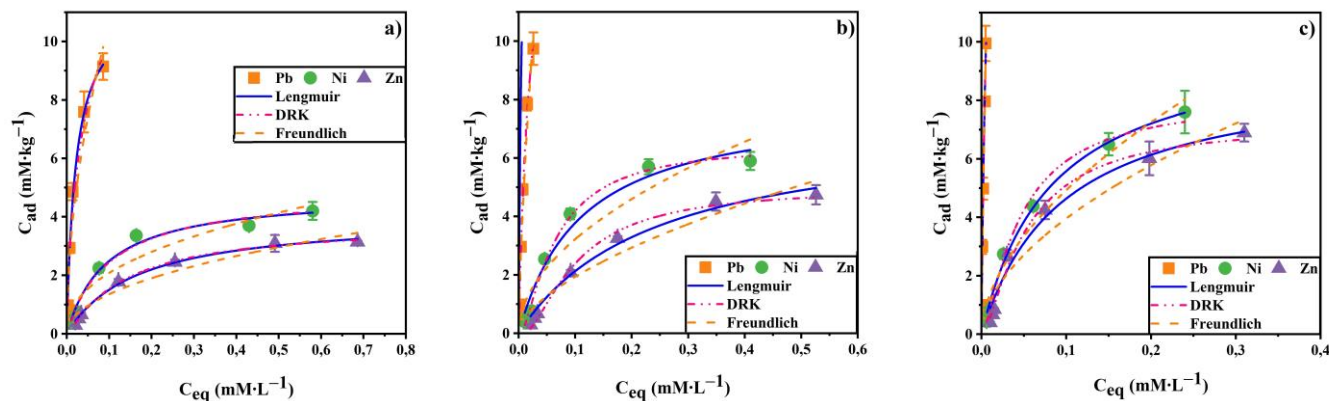


Figure 2. Individual adsorption isotherms for HMs by the Umbric Fluvisol (a), Gleyic Solonchak Sulfidic (b) and Haplic Chernozem (c)

Table 3. Individual adsorption isotherm parameters of HMs by Umbric Fluvisol, Gleyic Solonchak Sulfidic and Haplic Chernozem

Soil	Metal	Langmuir model				Dubinin-Radushkevich model			
		$K_L, \text{L} \cdot \text{mM}^{-1}$	$C_\infty, \text{mM} \cdot \text{kg}^{-1}$	$-\Delta G, \text{kJ} \cdot \text{M}^{-1}$	R^2	$C_\infty, \text{mM} \cdot \text{kg}^{-1}$	$E, \text{kJ} \cdot \text{M}^{-1}$	K	R^2
Umbric Fluvisol	Pb	46.79	11.51	9.53	0.992	11.13	4.29	8	0.981
	Ni	10.72	4.81	5.88	0.985	4.88	4.98	1	0.984
	Zn	6.01	4.02	4.44	0.995	3.71	4.44	1	0.998
Gleyic Solonchak Sulfidic	Pb	50.15	17.55	9.70	0.991	16.91	4.50	8	0.987
	Ni	9.01	7.97	5.45	0.964	8.90	4.45	1	0.969
	Zn	4.16	7.25	3.53	0.985	6.49	3.94	1	0.996
Haplic Chernozem	Pb	133.03	23.69	12.12	0.996	23.78	5.53	10	0.997
	Ni	12.20	10.16	6.20	0.996	11.35	5.06	1	0.997
	Zn	10.52	9.06	5.83	0.979	10.85	4.60	1	0.981

The isotherms depicting HM adsorption by soils exhibit a convex profile, a hallmark of Langmuir isotherms (Figure 2). The variations among these isotherms illuminate the unique adsorption capacities different soils possess for the HMs in question. At the initial phases of adsorption, the binding sites with the greatest interaction energy between sorbate and sorbent are swiftly occupied. As these prime sites become saturated, the binding strength decreases, and the amount of adsorbed substance diminishes. During this process, the nature of the sorption compounds formed changes – from inner-sphere complexes to outer-sphere ones (Sosorova et al., 2018). The specific transitions in HM-soil interaction mechanisms are intricately tied to the properties of the adsorbed cations. Across the concentration spectrum of the analyzed solutions (0.05–1.0 mM L⁻¹), all soil types exhibit a pronounced preference for Pb²⁺ over Ni²⁺ and Zn²⁺, a phenomenon evident in the contours of the isotherms and their alignment with the ordinate axis. In examining the isotherm approximation data via Equations (3) – (5), it became apparent that both the Langmuir and Dubinin-Radushkevich equations were adept at encapsulating the HM adsorption dynamics of the studied soils, whereas the Freundlich equation proved less fitting (Figure 2).

The investigation has unveiled that the C_∞ value for the examined soils diminishes in the following hierarchy: Pb²⁺ > Ni²⁺ ≥ Zn²⁺ (Table 3). In contrast, the KL value—reflective of the energetic interplay between the adsorbed cations and soil adsorption capacity (SAC)—exhibits a descending order of Pb²⁺ > Ni²⁺ > Zn²⁺. The adsorption potential of an ion appears to correlate tentatively with specific characteristics including hydrolyzability, electronegativity, and the softness parameter, as posited by Misono (1967). Notably, discrepancies in the computed parameters hinge predominantly on electronegativity values: Pb²⁺ at 2.33, followed by Ni²⁺ at 1.99, and Zn²⁺ trailing at 1.65 (McBride, 1994). Lead further boasts a superior softness metric (Pb²⁺ at 3.58, Ni²⁺ at 2.82, Zn²⁺ at 2.34), which influences the metal's affinity for soil entities, facilitating the establishment of covalent π-bonds (Basta and Sloan, 1999; Sposito, 2008; Shaheen et al., 2012). Additionally, the hydrolysis of metal ions is crucial to their soil adsorption dynamics. Abd-Elfattah and Wada (1981) identified the hydrolysis constant (pK₁) as a pivotal index of metal selectivity in soil contexts, with pK₁ values of 7.8 for Pb²⁺ and 9.9 for Ni²⁺ (Brown and Ekberg, 2016). Lower pK₁ values denote heightened interactions through the formation of inner-sphere complexes or sorption reactions (Park et al., 2016).

It has been noted that the Gibbs free energy (ΔG) derived from the Langmuir equation and the interaction energy of adsorbed heavy metals (HMs) with soil adsorption capacity (SAC) as calculated by the Dubinin-Radushkevich equation diverge markedly. In all instances, the adsorption energy derived from the Dubinin-Radushkevich equation was considerably lower (Table 3). Nonetheless, both models converge on a singular insight: the ranking of the analyzed metals, based on ΔG and E values, remains steadfast. The computed C_∞ values for the individual cations exhibit remarkable consistency across models, revealing no significant disparities (Table 3). Among the evaluated soils, the calculated values of C_∞ and KL adhere to the hierarchy: Haplic Chernozem > Gleyic Solonchak Sulfidic > Umbric Fluvisol. These variances largely stem from differences in soil texture, soil organic matter (SOM), exchangeable cations, and carbonate concentrations. In Umbric Fluvisol, these parameters are at their nadir, culminating in a diminished buffering capacity against heavy metals (Table 1, 3). The negative Gibbs free energy values (ΔG) (Table 3), ascertained through the Langmuir equation, affirm that the adsorption of HMs by soils unfolds as a spontaneous process, with ΔG directly proportional to KL: the higher the KL, the more pronounced the change in Gibbs energy.

Correlation analysis

Table 4 elegantly illustrates the correlation coefficients that intertwine various soil properties with sorption parameters (KL and C_∞) for the metals Pb, Ni, and Zn. These coefficients unveil the intricate relationships governing soil characteristics and metallic behavior.

Table 4. The correlation coefficients between K_L and C_∞ for each metal and selected soil characteristics

Metals	pH	CaCO ₃	SOM	Ca ²⁺	Mg ²⁺	ΣCa ²⁺ +Mg ²⁺	SiO ₂	Fe ₂ O ₃	Al ₂ O ₃	Physical clay (particle size <10 μm)	Clay (particle size <1 μm)
K_L											
Pb	-0.956	-0.430	0.991	0.702	-0.312	0.761	0.864	-0.534	0.614	0.843	0.741
Ni	-0.623	0.154	0.744	0.177	0.279	0.262	0.428	0.036	0.061	0.393	0.233
Zn	-0.814	-0.124	0.899	0.441	0.004	0.518	0.660	-0.240	0.333	0.631	0.491
C_∞											
Pb	-0.983	-0.801	0.938	0.953	-0.719	0.976	0.999	-0.866	0.911	0.909	0.968
Ni	-0.957	-0.862	0.895	0.980	-0.790	0.994	0.998	-0.915	0.950	0.891	0.990
Zn	-0.939	-0.889	0.868	0.990	-0.824	0.930	0.993	-0.937	0.967	0.995	0.911

For Pb^{2+} , KL exhibits a profound negative correlation with pH ($r = -0.956$) and a striking positive correlation with soil organic matter (SOM) ($r = 0.991$). Additional positive correlations are noted with $\Sigma\text{Ca}^{2+}+\text{Mg}^{2+}$ ($r = 0.761$), SiO_2 ($r = 0.864$), and particles smaller than $1 \mu\text{m}$ ($r = 0.741$). The C_{∞} value for Pb^{2+} mirrors this trend, revealing strong negative correlations with pH ($r = -0.983$) and CaCO_3 ($r = -0.801$), while displaying robust positive correlations with SOM ($r = 0.938$), Ca^{2+} ($r = 0.953$), and SiO_2 ($r = 0.999$).

For Ni^{2+} , KL reveals a moderate negative correlation with pH ($r = -0.623$) and a positive correlation with SOM ($r = 0.744$), though other correlations remain generally weak. The C_{∞} values for Ni^{2+} , however, showcase compelling negative correlations with pH ($r = -0.957$) and CaCO_3 ($r = -0.862$), alongside substantial positive correlations with SOM ($r = 0.895$), Ca^{2+} ($r = 0.980$), and $\Sigma\text{Ca}^{2+}+\text{Mg}^{2+}$ ($r = 0.994$).

For Zn^{2+} , KL displays a strong negative correlation with pH ($r = -0.814$) and a positive correlation with SOM ($r = 0.899$), though correlations with other soil properties are moderate. The C_{∞} values for Zn^{2+} reflect strong negative correlations with pH ($r = -0.939$) and CaCO_3 ($r = -0.889$), as well as significant positive correlations with SOM ($r = 0.868$), Ca^{2+} ($r = 0.990$), and $\Sigma\text{Ca}^{2+}+\text{Mg}^{2+}$ ($r = 0.930$). Notably, a striking positive correlation emerges with the content of particles smaller than $10 \mu\text{m}$ ($r = 0.995$).

The sorption parameters of soils regarding heavy metals are predominantly shaped by pH, soil organic matter (SOM), and clay content. At diminished pH levels, numerous metallic ions manifest as cations, displaying an increased affinity for adsorption onto negatively charged soil particles. Conversely, elevated pH levels may hinder this process; here, the formation of hydroxide complexes occurs, yielding compounds less susceptible to adsorption. The role of SOM is intricately tied to its organic functional groups, notably carboxyl and phenolic entities, which adeptly bind metal cations, thereby enhancing the likelihood of complex formations. Furthermore, clay minerals, with their expansive specific surface area and considerable cation exchange capacity, significantly boost the adsorption of metals within the soil matrix (Bradl, 2004). In essence, these intertwined factors create a dynamic interplay, dictating the availability and mobility of heavy metals in the soil environment, ultimately impacting their ecological fate.

Adsorption kinetics

The kinetic data were meticulously analyzed to ascertain both the rate of adsorption and its nature—whether it be chemisorption or physisorption. The influence of contact time on heavy metals (HMs) adsorption by soils is illustrated in Figure 3.

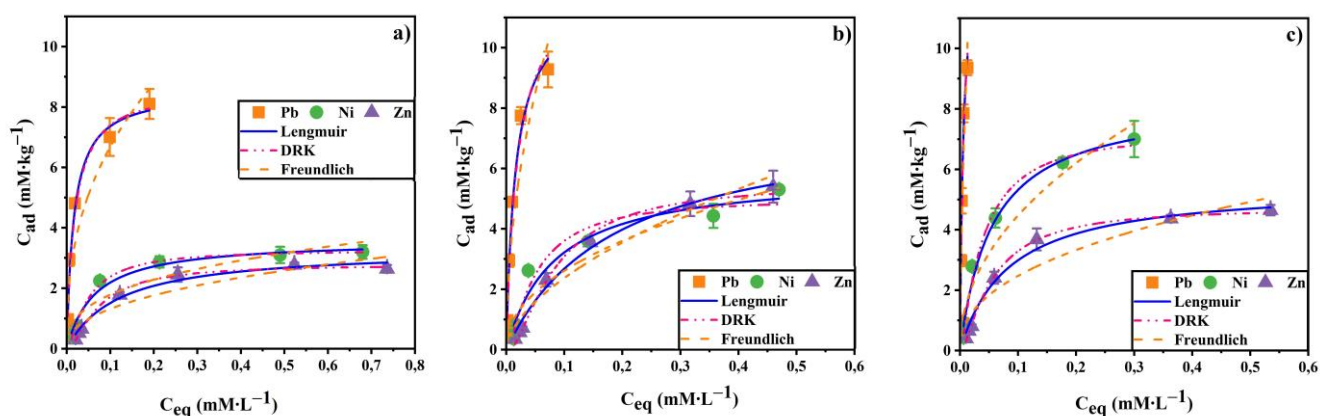


Figure 3. Kinetics of individual adsorption for HMs by Umbric Fluvisol (a), Gleyic Solonchac Sulfidic (b) and Haplic Chernozem (c)

To elucidate the findings, nonlinear statistical analysis was employed to adeptly fit Eqs. (8) and (9) to the experimental kinetic data, as detailed in Table 5. Notably, the quantity of adsorbed HMs escalated in tandem with contact time (see Figure 3). This adsorption process exhibited a notably rapid rate, achieving equilibrium within the observed timeframe of a day. After three hours, the curves began to level off, signifying a negligible change in the quantity of metals absorbed by the soil over time. This behavior may be ascribed to the profusion of active sites on the soil surface that initially facilitate swift sorption. However, as these sites gradually become occupied, the rate of sorption slows, reflecting the intricate interplay between time and the dynamic availability of adsorption sites.

The findings illuminate the intricate dynamics of heavy metal ion adsorption by soils, unfolding in two distinct stages. The initial phase is a swift dance of rapid surface adsorption, predominantly driven by the magnetic pull of electrostatic attraction and ion exchange (Mouni et al., 2009). This is succeeded by a more

languid stage, potentially characterized by the diffusion of ions into the soil's granular embrace (Karavanova and Schmidt, 2001). Data summarized in Table 3 affirm that the pseudo-second order equation most aptly captures the essence of the sorption process, with R^2 values soaring high between 0.914 and 0.965, a stark contrast to the subdued values of the pseudo-first order model, which languish between 0.597 and 0.760 (Table 5). This analysis underscores chemisorption as the rate-limiting step, relegating diffusion to a role of little consequence.

At equilibrium, the K_2 values delineate a hierarchy of sorption rates: Pb^{2+} reigns supreme over Zn^{2+} and Ni^{2+} in both Umbric Fluvisol and Haplic Chernozem, while in Gleyic Solonchac Sulfidic, Zn^{2+} commands attention with Pb^{2+} closely trailing. Notably, the sorption capacity (Q_e) for Pb^{2+} consistently eclipses that of Zn^{2+} and Ni^{2+} across all examined soils (Table 5).

Table 5. Kinetic model parameters of the HMs adsorption by studied soils

Soil	Metal	Q_e , mM·kg ⁻¹	PFO model		PSO model	
			R^2	K_1 , min ⁻¹	R^2	K_2 , kg·mM ⁻¹ ·min ⁻¹
Umbric Fluvisol	Pb	4.754	0.597	0.0034	0.952	0.0481
	Ni	3.572	0.646	0.0032	0.942	0.0352
	Zn	3.090	0.760	0.0032	0.903	0.0427
Gleyic Solonchac Sulfidic	Pb	4.925	0.655	0.0033	0.943	0.0379
	Ni	4.157	0.647	0.0034	0.938	0.0377
	Zn	3.262	0.539	0.0039	0.923	0.0641
Haplic Chernozem	Pb	4.992	0.608	0.0035	0.936	0.0431
	Ni	4.404	0.741	0.0032	0.936	0.0257
	Zn	4.021	0.720	0.0032	0.915	0.0346

Competitive adsorption of HMs by soils

Adsorption isotherms

The principal force that governs the sorption of heavy metal cations by the examined soils, when subjected to solutions containing all three cations simultaneously, is their inherent competition for limited sorption sites. In the realm of competitive adsorption, the soils consistently exhibit a diminished sorption capacity with escalating initial heavy metal concentrations (Figure 4), a phenomenon amplified in contrast to mono-element adsorption. The efficiency of adsorption for each metal unfolds as follows: Pb^{2+} – 81.02-99.00%; Ni^{2+} – 32.00-93.00%; Zn^{2+} – 26.40-81.25%. The overarching absorption capacity is hierarchically ordered as: Haplic Chernozem > Gleyic Solonchac Sulfidic > Umbric Fluvisol.

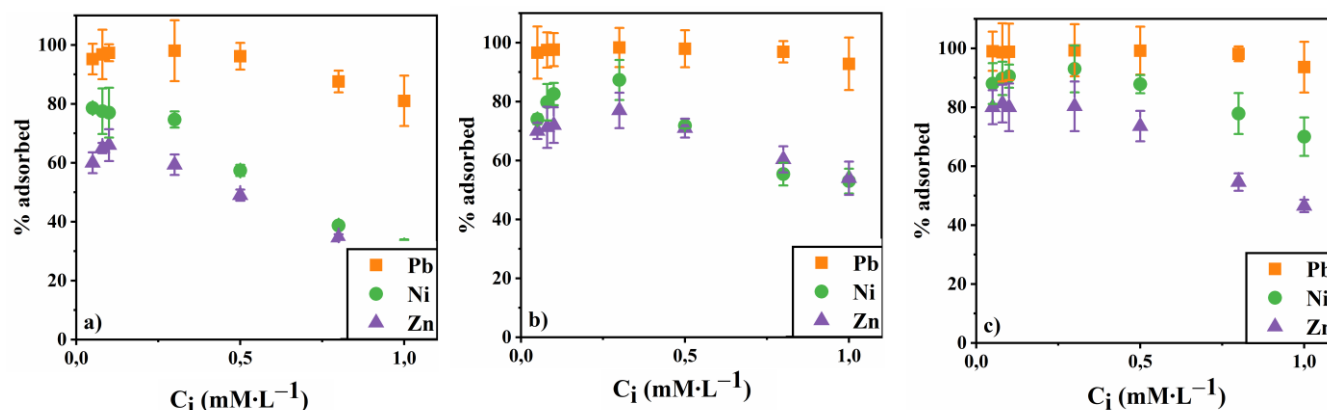


Figure 4. The efficiency of HMs adsorption (% adsorbed) by the Umbric Fluvisol (a), Gleyic Solonchac Sulfidic (b) and Haplic Chernozem (c) during polyelement pollution

Figure 5 elucidates the sorption isotherms of Pb^{2+} , Ni^{2+} , and Zn^{2+} within multi-metal solutions. Given the constrained sorption capacities during polycationic adsorption, the energy associated with each cation, articulated through the constant K_1 , rises, while the peak adsorption (C_∞) wanes compared to mono-element scenarios (Tables 3, 6). This trend elucidates the competitive dynamics hindering the adsorption of individual ions. Furthermore, the interplay between adsorption sites and ion competition substantially diminishes overall adsorption capacity. Thus, the governing mechanisms of interaction for Pb^{2+} , Ni^{2+} , and Zn^{2+} with the studied soils persist consistently across both mono-element and poly-element sorption processes.

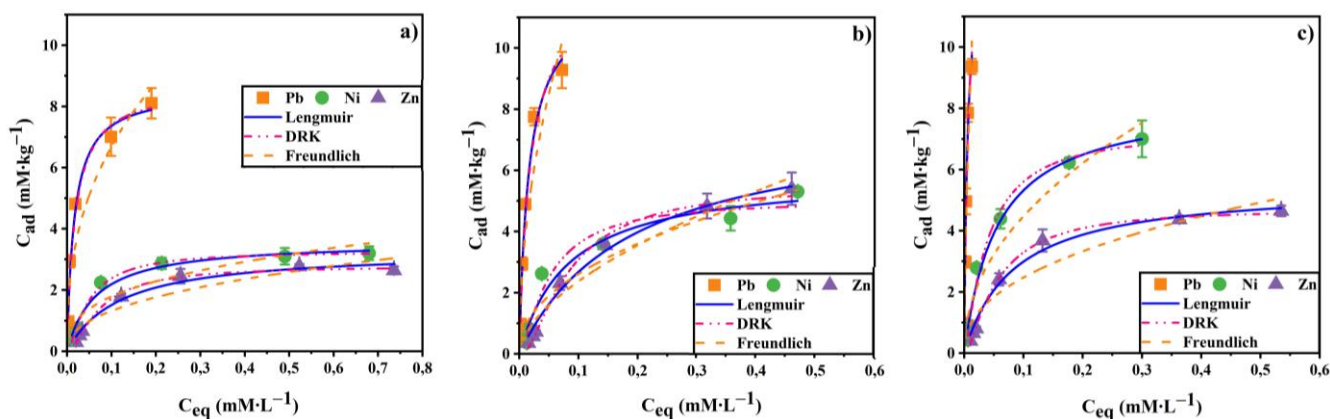


Figure 5. Competitive adsorption isotherms for HMs by the Umbric Fluvisol (a), Gleyic Solonchac Sulfidic (b) and Haplic Chernozem (c)

Table 6. Competitive adsorption isotherm parameters of HMs by studied soils

Soil	Metal	Langmuir equation model				Dubinin-Radushkevich model			
		K_L , L·mM ⁻¹	C_∞ , mM·kg ⁻¹	$-\Delta G$, kJ·M ⁻¹	R^2	C_∞ , mM·kg ⁻¹	E , kJ·M ⁻¹	K	R^2
Umbric Fluvisol	Pb	61.64	8.56	10.21	0.978	8.34	3.73	15	0.962
	Ni	15.59	3.59	6.80	0.980	3.84	5.30	1	0.971
	Zn	8.47	3.30	5.29	0.979	3.35	4.57	1	0.983
Gleyic Solonchac Sulfidic	Pb	62.41	11.78	10.24	0.978	11.43	3.74	15	0.951
	Ni	12.14	5.87	6.19	0.952	5.32	3.13	5	0.952
	Zn	5.34	7.70	4.15	0.989	7.15	4.23	1	0.995
Haplic Chernozem	Pb	173.48	14.06	12.77	0.978	13.78	4.23	30	0.960
	Ni	17.90	8.30	7.15	0.987	8.84	4.61	2	0.984
	Zn	12.05	5.48	6.17	0.986	5.87	4.96	1	0.984

In the intricate dance of competition among three metal ions, the inherent properties of these metals profoundly influence their sorption capabilities within the embrace of soil. Across all soil types, the affinity for Pb²⁺ stands out markedly, eclipsing that of its counterparts. When these metals vie for a common adsorption site, the resilient Pb²⁺ can displace Ni²⁺, which in turn may usurp Zn²⁺ position. This dynamic interplay reveals a deeper truth: the presence of competing ions compels an increase in the bond strength between metals and soil particles, thereby diminishing the overall absorption capacity compared to scenarios involving single-component systems.

Adsorption kinetics

The dynamics of competitive heavy metal (HM) adsorption are revealed in Figure 6. The sorption capacity of these metals (Q_e) diminishes with their simultaneous introduction into the examined soils, in stark contrast to the singular adsorption of each metal, as illustrated in Figure 6. Such trends align seamlessly with the adsorption isotherms, rooted in the competition for active sorption sites within the soil matrix. This phenomenon may stem from the repulsive electrostatic forces that arise among the three ions present in multi-element systems. Notably, Pb²⁺ exhibits the most favorable sorption rates, signifying its greater affinity over Ni²⁺ and Zn²⁺, which present similar data profiles.

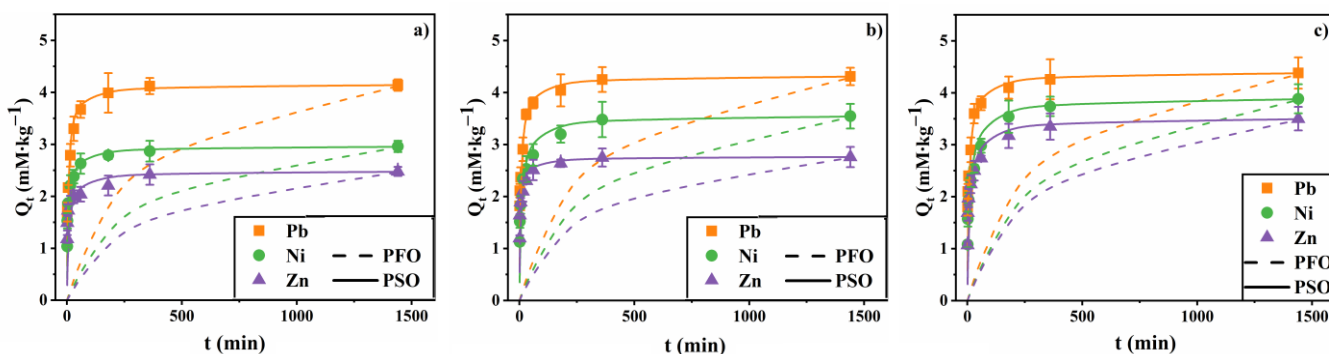


Figure 6. Kinetics of competitive HMs adsorption by Umbric Fluvisol (a), Gleyic Solonchac Sulfidic (b) and Haplic Chernozem (c)

The correlation coefficients (R^2) reinforce this finding, showcasing elevated values for the pseudo-second order (0.922-0.974) compared to the pseudo-first order (0.580-0.753). Additionally, the K_2 value constants (Table 7) reveal marginally lower figures (0.0201-0.0626), suggesting a slight extension of time necessary to reach equilibrium. This observation can be attributed to the intensified competition for active sites, which leads to a deceleration in the adsorption process.

Table 7. Kinetic model parameters of the competitive HMs adsorption by studied soils

Soil	Metal	Q_e , mM·kg ¹	PFO model		PSO model	
			R^2	K_1 , min ⁻¹	R^2	K_2 , kg·mM ⁻¹ ·min ⁻¹
Umbric Fluvisol	Pb	4.157	0.641	0.0033	0.968	0.0374
	Ni	2.965	0.580	0.0036	0.973	0.0479
	Zn	2.488	0.679	0.0032	0.922	0.0537
Gleyic Solonchak Sulfidic	Pb	4.324	0.641	0.0033	0.957	0.0391
	Ni	3.565	0.716	0.0031	0.957	0.0260
	Zn	2.764	0.585	0.0037	0.964	0.0626
Haplic Chernozem	Pb	4.386	0.623	0.0039	0.974	0.0267
	Ni	3.909	0.753	0.0031	0.949	0.0201
	Zn	3.513	0.709	0.0034	0.943	0.0243

Conclusion

The physicochemical, mineralogical, and sorption characteristics of coastal soils from the Lower Don region and the Taganrog Bay coast in southern Russia were meticulously examined. This study delved into the individual and competitive sorption processes of heavy metals Pb²⁺, Ni²⁺, and Zn²⁺, employing sorption isotherms to unveil the underlying interactions within these soils. In every instance, the sorption phenomena were aptly encapsulated by the Langmuir model. The resulting sorption isotherms delineated a hierarchy of metal affinity: Pb > Ni > Zn, and illuminated distinct soil types: Haplic Chernozem > Gleyic Solonchak Sulfidic > Umbric Fluvisol. Experiments on the competitive sorption of heavy metals unveiled variable selective sorption sites among the soils for each metal; lead emerged as the predominant adsorbate, while nickel and zinc exhibited diminished adsorption under competitive conditions. Correlation analysis underscored the pivotal roles of pH, soil organic matter, and clay content in facilitating heavy metal adsorption. Notably, the pseudo-second-order kinetic model emerged as a superior descriptor of the adsorption dynamics, emphasizing chemisorption as the rate-limiting step, with diffusion playing a subordinate role. These insights underscore the urgent need for effective strategies to combat heavy metal pollution and safeguard coastal ecosystems.

Acknowledgments

The study was carried out with the financial support of the Russian Science Foundation, Russian Federation, project no. 20-14-00317.

References

- Abd-Elfattah, A., Wada, K., 1981. Adsorption of lead, copper, zinc, cobalt, and cadmium by soils that differ in cation-exchange materials. *European Journal of Soil Science* 32(2): 271-283.
- Akrawi, H., Al-Obaidi, M., Abdulrahman, C.H., 2021. Evaluation of Langmuir and Freundlich isotherm equation for Zinc Adsorption in some calcareous soil of Erbil province north of Iraq. *IOP Conference Series: Earth and Environmental Science* 76(1): 012017.
- Bai, J., Zhao, Q., Wang, W., Wang, X., Jia, J., Cui, B., Liu, X., 2019. Arsenic and heavy metals pollution along a salinity gradient in drained coastal wetland soils: depth distributions, sources and toxic risks. *Ecological indicators* 96: 91-98.
- Basta, N., Sloan, J., 1999. Bioavailability of heavy metals in strongly acidic soils treated with exceptional quality biosolids. *Journal of Environmental Quality* 28(2): 633-638.
- Bauer, T., Pinski, D., Minkina, T., Nevidomskaya, D., Mandzhieva, S., Burachevskaya, M., Chaplygin, V., Popileshko, Y., 2018. Time effect on the stabilization of technogenic copper compounds in solid phases of Haplic Chernozem. *Science of the Total Environment* 626: 1100-1107.
- Bauer, T.V., Pinski, D.L., Minkina, T.M., Shuvaeva, V.A., Soldatov, A.V., Mandzhieva, S.S., Tsitsuashvili, V.S., Nevidomskaya, D.G., Semenov, I.N., 2022. Application of XAFS and XRD methods for describing the copper and zinc adsorption characteristics in hydromorphic soils. *Environmental Geochemistry and Health* 44(2): 335-347.
- Bradl, H.B., 2004. Adsorption of heavy metal ions on soils and soils constituents. *Journal of Colloid and Interface Science* 277(1): 1-18.

- Brown, P.L., Ekberg, C., 2016. Hydrolysis of metal ions. John Wiley and Sons, Weinheim, Germany. 917p.
- Burachevskaya, M., Minkina, T., Bauer, T., Lobzenko, I., Fedorenko, A., Mazarji, M., Sushkova, S., Mandzhieva, S., Nazarenko, A., Butova, V., 2023. Fabrication of biochar derived from different types of feedstocks as an efficient adsorbent for soil heavy metal removal. *Scientific Reports* 13: 2020.
- Cao, W., Qin, C., Zhang, Y., Wei, J., Shad, A., Qu, R., Xian, Q., Wang, Z., 2024. Adsorption and migration behaviors of heavy metals (As, Cd, and Cr) in single and binary systems in typical Chinese soils. *Science of the Total Environment* 950: 175253.
- Chizhikova, N., Khitrov, N., Varlamov, E., Churilin, N., 2018. The profile distribution of minerals within the solonetz in Yergeni. *Dokuchaev Soil Bulletin* 91: 63-84.
- Cui, X., Hao, H., Zhang, C., He, Z., Yang, X., 2016. Capacity and mechanisms of ammonium and cadmium sorption on different wetland-plant derived biochars. *Science of the Total Environment* 539: 566-575.
- Daramola, S., Demlie, M., Hingston, E., 2024. Mineralogical and sorption characterization of lateritic soils from Southwestern Nigeria for use as landfill liners. *Journal of Environmental Management* 355: 120511.
- Das, B., Mondal, N., Bhaumik, R., Roy, P., 2014. Insight into adsorption equilibrium, kinetics and thermodynamics of lead onto alluvial soil. *International Journal of Environmental Science and Technology* 11: 1101-1114.
- Degryse, F., Smolders, E., Parker, D., 2009. Partitioning of metals (Cd, Co, Cu, Ni, Pb, Zn) in soils: concepts, methodologies, prediction and applications—a review. *European journal of Soil Science* 60(4): 590-612.
- Diagboya, P.N., Olu-Owolabi, B.I., Adebowale, K.O., 2015. Effects of time, soil organic matter, and iron oxides on the relative retention and redistribution of lead, cadmium, and copper on soils. *Environmental Science and Pollution Research* 22: 10331-10339.
- Fisher-Power, L.M., Cheng, T., Rastghalam, Z.S., 2016. Cu and Zn adsorption to a heterogeneous natural sediment: Influence of leached cations and natural organic matter. *Chemosphere* 144: 1973-1979.
- Ho, Y.-S., McKay, G., 1999. Pseudo-second order model for sorption processes. *Process biochemistry* 34(5): 451-465.
- Hobson, J.P., 1969. Physical adsorption isotherms extending from ultrahigh vacuum to vapor pressure. *The Journal of Physical Chemistry* 73(8): 2720-2727.
- Imoto, Y., Yasutaka, T., 2020. Comparison of the impacts of the experimental parameters and soil properties on the prediction of the soil sorption of Cd and Pb. *Geoderma* 376: 114538.
- ISO 10390:2005. Soil quality — Determination of pH. Available at [Access date: 21.04.2024]: <https://www.iso.org/obp/ui/#iso:std:iso:10390:ed-2:v1:en>
- ISO 10693:1995. Soil quality — Determination of carbonate content — Volumetric method. Available at [Access date: 21.04.2024]: <https://www.iso.org/obp/ui/#iso:std:iso:10693:ed-1:v1:en>
- ISO 14235:1998. Soil quality — Determination of organic carbon by sulfochromic oxidation. Available at [Access date: 21.04.2024]: <https://www.iso.org/obp/ui/#iso:std:iso:14235:ed-1:v1:en>
- ISO 23470:2018. Soil quality — Determination of effective cation exchange capacity (CEC) and exchangeable cations using a hexamminecobalt(III)chloride solution. Available at [Access date: 21.04.2024]: <https://www.iso.org/obp/ui/#iso:std:iso:23470:ed-2:v1:en>
- IUSS, 2015. World reference base for soil resources 2014 International soil classification system for naming soils and creating legends for soil maps. Update 2015. World Soil Resources Reports 106. Food and Agriculture Organization of the United Nations (FAO), Rome, Italy. 192p. Available at [Access date: 21.04.2024]: <http://www.fao.org/3/i3794en/i3794en.pdf>
- Jalali, M., Moharrami, S., 2007. Competitive adsorption of trace elements in calcareous soils of western Iran. *Geoderma* 140(1-2): 156-163.
- Karavanova, E.I., Schmidt S.Yu., 2001. Sorption of water-soluble copper and zinc compounds by forest litter. *Eurasian Soil Science* 34(9): 967-974.
- Komuro, R., Kikumoto, M., 2024. IntraPD model: Leaching of heavy metals from naturally contaminated soils. *Environmental Pollution* 340: 122861.
- Konstantinova, E., Minkina, T., Nevidomskaya, D., Lychagin, M., Bezberdaya, L., Burachevskaya, M., Rajput, V. D., Zamulina, I., Bauer, T., Mandzhieva, S., 2024. Potentially toxic elements in urban soils of the coastal city of the Sea of Azov: Levels, sources, pollution and risk assessment. *Environmental Research* 252: 119080.
- Konstantinova, E., Minkina, T., Nevidomskaya, D., Mandzhieva, S., Bauer, T., Zamulina, I., Voloshina, M., Lobzenko, I., Maksimov, A., Sushkova, S., 2023. Potentially toxic elements in surface soils of the Lower Don floodplain and the Taganrog Bay coast: sources, spatial distribution and pollution assessment. *Environmental Geochemistry and Health* 45(1): 101-119.
- Kravchenko, E., Sushkova, S., Raza, M. H., Minkina, T., Dudnikova, T., Barbashev, A., Maksimov, A., Wong, M.H., 2024. Ecological and human health impact assessments based on long-term monitoring of soil PAHs near a coal-fired power plant. *Environmental Geochemistry and Health* 46: 288.
- Kulp, S.A., Strauss, B.H., 2019. New elevation data triple estimates of global vulnerability to sea-level rise and coastal flooding. *Nature Communications* 10: 4844.
- Li, Y., Liu, J., Wang, Y., Tang, X., Xu, J., Liu, X., 2023. Contribution of components in natural soil to Cd and Pb competitive adsorption: semi-quantitative to quantitative analysis. *Journal of Hazardous Materials* 441: 129883.

- Liu, H., Xie, J., Cheng, Z., Wu, X., 2023. Characteristics, chemical speciation and health risk assessment of heavy metals in paddy soil and rice around an abandoned high-arsenic coal mine area, Southwest China. *Minerals* 13(5): 629.
- Lu, S., Xu, Q., 2009. Competitive adsorption of Cd, Cu, Pb and Zn by different soils of Eastern China. *Environmental Geology* 57: 685-693.
- McBride, M.B., 1994. Environmental chemistry of Soils. Oxford University Press. 406p.
- Misono, M., Ochiai, E., Saito, Y., Yoneda, Y., 1967. A new dual parameter scale for the strength of Lewis acids and bases with the evaluation of their softness. *Journal of Inorganic and Nuclear Chemistry* 29(11): 2685-2691.
- Mouni, L., Merabet, D., Robert, D., Bouzaza, A., 2009. Batch studies for the investigation of the sorption of the heavy metals Pb²⁺ and Zn²⁺ onto Amizour soil (Algeria). *Geoderma* 154(1-2): 30-35.
- Najamuddin, Inayah, Labenua, R., Samawi, M.F., Yaqin, K., Paembonan, R.E., Ismail, F., Harahap, Z.A., 2024. Distribution of heavy metals Hg, Pb, and Cr in the coastal waters of small islands of Ternate, Indonesia. *Ecological Frontiers* 44(3): 529-537.
- Park, J.-H., Ok, Y.S., Kim, S.-H., Cho, J.-S., Heo, J.-S., Delaune, R.D., Seo, D.-C., 2016. Competitive adsorption of heavy metals onto sesame straw biochar in aqueous solutions. *Chemosphere* 142: 77-83.
- Pinskii, D., Shary, P., Mandzhieva, S., Minkina, T., Perelomov, L., Maltseva, A., Dudnikova, T., 2023. Effect of composition and properties of soils and soil-sand substrates contaminated with copper on morphometric parameters of barley plants. *Eurasian Soil Science* 56(3): 352-362.
- Shaheen, S.M., Derbalah, A.S., Moghanm, F., 2012. Removal of heavy metals from aqueous solution by zeolite in competitive sorption system. *International Journal of Environmental Science and Development* 3(4): 362-367.
- Shein, E., 2009. The particle-size distribution in soils: problems of the methods of study, interpretation of the results, and classification. *Eurasian Soil Science* 42: 284-291.
- Sipos, P., Németh, T., Kis, V.K., Mohai, I., 2008. Sorption of copper, zinc and lead on soil mineral phases. *Chemosphere* 73(4): 461-469.
- Sosorova, S.B., Merkusheva, M.G., Boloneva, L.N., Ubuguno, L.L., 2018. Parameters of sorption of cobalt and nickel ions by salt marshes of Western Transbaikal. *Agrochemistry* 9: 69-79. [In Russian]
- Sposito, G., 2008. The chemistry of soils. Second edition. Oxford university press, USA. 329p.
- Tepanosyan, G., Sahakyan, L., Belyaeva, O., Asmaryan, S., Saghatelyan, A., 2018. Continuous impact of mining activities on soil heavy metals levels and human health. *Science of the Total Environment* 639: 900-909.
- Umeh, T.C., Nduka, J.K., Akpomie, K.G., 2021. Kinetics and isotherm modeling of Pb (II) and Cd (II) sequestration from polluted water onto tropical ultisol obtained from Enugu Nigeria. *Applied Water Science* 11: 65.
- Usman, A.R.A., 2008. The relative adsorption selectivities of Pb, Cu, Zn, Cd and Ni by soils developed on shale in New Valley, Egypt. *Geoderma* 144(1-2): 334-343.
- Vega, F.A., Covelo, E.F., Andrade, M., 2006. Competitive sorption and desorption of heavy metals in mine soils: influence of mine soil characteristics. *Journal of Colloid and Interface Science* 298(2): 582-592.
- Vodyanitskii, Y.N., Rogova, O., Pinskii, D.L., 2000. Application of the Langmuir and Dubinin-Radushkevich equations to the description of Cu and Zn adsorption in rendzinas. *Eurasian Soil Science* 33(11): 1226-1233.
- Ward, N.D., Megonigal, J.P., Bond-Lamberty, B., Bailey, V.L., Butman, D., Canuel, E.A., Diefenderfer, H., Ganju, N.K., Goñi, M.A., Graham, E.B., Hopkinson, C.S., Khangaonkar, T., Langley, J.A., McDowell, N.G., Myers-Pigg, A.N., Neumann, R.B., Osburn, C.L., Price, R.M., Rowland, J., Sengupta, A., Simard, M., Thornton, P.E., Tzortziou, M., Vargas, R., Weisenhorn, P.B., Windham-Myers, L., 2020. Representing the function and sensitivity of coastal interfaces in Earth system models. *Nature Communications* 11(1): 2458.
- Yu, D., Wang, Y., Ding, F., Chen, X., Wang, J., 2021. Comparison of analysis methods of soil heavy metal pollution sources in China in last ten years. *Chinese Journal of Soil Science* 52(4): 1000.
- Zamora-Ledezma, C., Negrete-Bolagay, D., Figueroa, F., Zamora-Ledezma, E., Ni, M., Alexis, F., Guerrero, V.H., 2021. Heavy metal water pollution: A fresh look about hazards, novel and conventional remediation methods. *Environmental Technology and Innovation* 22: 101504.
- Zwolak, A., Sarzyńska, M., Szpyrka, E., Stawarczyk, K., 2019. Sources of soil pollution by heavy metals and their accumulation in vegetables: A review. *Water, Air, and Soil Pollution* 230: 164.